Synthesis of a Bone Like Composite Material Dderived from Natural Pearl Oyster Shells for Potential Tissue Bioengineering Applications

Ravi Krishna Brundavanam, Derek Fawcett, and Gérard Eddy Jai Poinern
Murdoch Applied Nanotechnology Research Group, Department of Physics, Energy Studies and Nanotechnolog,
School of Engineering and Energy, Murdoch University, Murdoch, Western Australia 6150, Australia
Email: ravikrishna_brundavanam@yahoo.com, {d.fawcett, g.poinern}@murdoch.edu.au

***Abstract*—Hydroxyapatite is generally considered a viable substitute for bone in a number of medical and dental procedures such as bone repair, bone augmentation and coating metal implants. Unfortunately, hydroxyapatites poor mechanical properties make it unsuitable for many load bearing applications. In this work various grades of finely crushed *Pinctada maxima* (pearl oyster shell) were combined with a nanometre scale hydroxyapatite powder to form novel composite materials. A comparative study was made between the various powder based composites synthesized. The crystalline structure and morphology of the various powder based composites were investigated using X-ray diffraction and field emission scanning electron microscopy. Also examined was a number of techniques for depositing hydroxyapatite directly onto oyster shell substrates.**

***Index Terms*—nano-hydroxyapatite, biocompatible, ultrasonic irradiation, oyster shells**

I. Introduction

The human skeletal system is essential for support and movement of the body. An important structural material forming the skeletal system is an organic-inorganic composite called bone. This natural composite is composed of proteins in the form of collagen fibrils and macromolecules like proteoglycans that are all embedded in a well arrayed inorganic crystalline hydroxyapatite (HAP) matrix [1, 2]. It is this remarkable combination and distribution of constituent materials that gives bone its unique mechanical properties and its ability to withstand various mechanical and structural loads encountered during daily physical activity. HAP is a mineral composed of calcium and phosphate ions and has the general formula of $[Ca_{10}(OH)_2(PO_4)_6]$. The close chemical similarity between synthetic HAP and HAP naturally found in bone has led to an extensive research effort focused on using synthetic HAP as a viable bone replacement material in a number of clinical procedures [3], [4]. Unfortunately, due to HAPs low mechanical strength its use has been restricted to low load bearing applications. In a number of cases, its deficiencies have been improved by combining it with other materials. For example, materials such as high density polyethylene and polypropylene have been successfully combined with HAP to improve its load bearing capabilities [5], [6].

Alternatively, other researchers have gone back to nature to look for a more effective ways of producing biosynthetic materials and composites for potential tissue engineering applications. Seashells are naturally occurring ceramic composites that are dense, hard, and remarkably robust. The shell structure has a number of highly desirable mechanical properties that enable it to protect the soft body of the animal against environmental damage and predators. Shells are brittle or quasi-brittle materials composed of mineral components (~95%) and proteins (~5%). It is this compositional blend that gives a shell its high degree of stiffness and hardness. However, it is shell toughness and its ability to resist crack propagation that has attracted considerable interest [7], [8]. This interest stems from the observation that shell fracture toughness can be two to three orders of magnitude greater than the toughness of individual shell components [9], [10]. Another interesting feature is the much larger mechanical strain shells have at failure compared to manmade ceramics [8].

Nacre is the inner iridescent layer found in *Pinctada maxima* (pearl oyster shell) and similar shells such as abalone. Nacre is composed of a crystalline $CaCO_3$ mineral phase (aragonite) suspended in an organic matrix. The aragonite is in the form of polygon shaped tablets ranging in size from 5 to15 μm in diameter and 0.5 to 1 μm in thickness that are stacked into a three dimensional brick wall-like structure. The wall-like structures can consist of columns or sheets depending on the species and typically forms 95% of the composite. Pearl oyster shells have a sheet-like structure. Recent atomic force microscopy studies have shown the individual tablets are suspended in an organic matrix of proteins and polysaccharides. The organic matrix makes up the remaining 5% of the composite [11], [12]. Besides the highly advantageous mechanical properties, the nacre is biologically compatible with bone tissues [13], [14]. Because of the promising mechanical and biocompatibility properties, nacre is a prime candidate for potential tissue engineering applications. For example,

Manuscript received August 26, 2016; revised March 15, 2017.

doi: 10.18178/jomb.6.1.29-34

recent animal *in vivo* studies by Berland et al. have shown good cellular interaction between nacre implants and bone forming cells [15]. From another perspective, Vecchio et al. have been able to converted *Strombus gigas* (conch) and *Tridacna gigas* (Giant clam) shells to HAP while preserving their original dense columnar structure [16].

This article reports on the use of HAP and $CaCO_3$ derived from oyster shells to form novel HAP/$CaCO_3$ composites and HAP surface coatings on nacre. The first part of the article reports on the crystalline structure and morphology of synthesized nanometre scale HAP powders. The second part examines the use of shell derived $CaCO_3$ that still retains properties of the shell to manufacture HAP/$CaCO_3$ composites. And thirdly, we report on the use of HAP surface coating on nacre substrates to improve biocompatibility and overcome poor mechanical properties inherent with pure HAP constructs.

II. Materials and Methods

A. Materials

All chemicals used in this work were supplied by Chem-Supply (Australia) and all aqueous solutions were made using Milli-Q® water (18.3 MΩ cm^{-1}) produced by an ultrapure water system (Barnstead Ultrapure Water System D11931; Thermo Scientific, Dubuque, IA). *Pinctada Maxima* (pearl oyster) shells were supplied raw and were prepared as specified in section 2.3.

B. Preparation of Nanometre Scale HAP Powders

A detailed description of the HAP synthesis process developed by the authors can be found in the literature [17, 18]. For completeness, a brief procedural description is outlined as follows. The procedure begins by first adding a 40 mL solution of 0.32 M calcium nitrate tetra-hydrate into a small glass beaker and then adjusting the solution pH to 9.0 using approximately 2.5 mL of ammonium hydroxide. The solution is then sonicated using a Hielscher Ultrasound Processor UP50H set at 50 W and maximum amplitude for 1 h. During a second hour of sonication 60 mL of 0.19 M potassium di-hydrogen phosphate solution was slowly added while the solution pH was maintained at 9.0 and the Calcium/Phosphate [Ca/P] ratio was maintained at 1.67. At the end of the second sonication period, the solution was centrifuged (15,000 g) for 20 minutes at room temperature to produce a precipitate. The precipitate was collected, washed and centrifuged for a further 10 minutes before being placed into a ceramic boat ready for heat treatment. The heat treatment consisted of placing a sample loaded ceramic boat into an electric tube furnace. The reaction temperatures used were either 300°C or 400°C and the reaction time period was 2 hours for temperatures. After thermal treatment, the agglomerated samples were milled to form an ultrafine HAP powder. A schematic of the synthesis process is presented in Fig. 1.

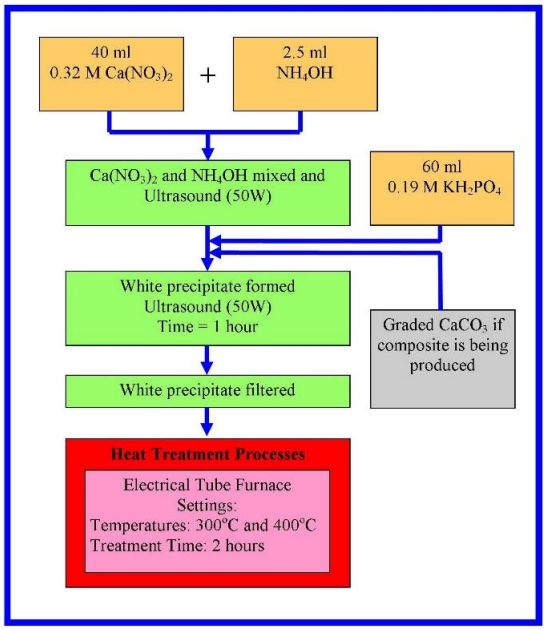

Figure 1. Schematic of synthesis process for producing HAP and HAP/$CaCO_3$ composites.

C. Preparation of HAP Based Calcium Carbonate Composite Powders

$CaCO_3$ was derived from *Pinctada Maxima* (pearl oyster) shells. The shells were first washed and scrubbed to removal all traces of organic matter. This was followed by giving the shells a final wash down using Milli-Q® water and then allowing them to air dry before being stored for the next stage of process. Shell material was used in two forms. In the first form shells underwent milling to produce $CaCO_3$ powders of varying grades. A metallurgical ring crusher was used to crush and grind the shells into a powder. After grinding, a *Roto-Tap* was used for 30 minute to sieve the powder. Sieving produce a variety of powder grades ranging from 38 to 850 micrometers as seen in Fig. 2. In the second form shells were cut into 1 cm^2 test substrates.

Preparation of the HAP/$CaCO_3$ composites started by selecting the appropriate $CaCO_3$ grade and then weighing out the required mass. In this case the mass percentages of $CaCO_3$ selected were 5% and 10%, with the remaining mass balance made up of HAP powder. However, before being incorporated into the HAP synthesis process the $CaCO_3$ powders were bleached for 30 minutes. The bleached $CaCO_3$ was then added to the HAP processing procedure to produce the required blend as seen in Fig. 1. Visual inspection during processing and after heat treatment revealed a noticeable difference between pure HAP powders, pure $CaCO_3$ powders and the respective HAP/$CaCO_3$ powder blends. However, differences between the 5% and 10% $CaCO_3$ blends were much harder to distinguish and could only be differentiated under electron microscopy. Fig. 3 presents a representative image of a 10% $CaCO_3$ blend.

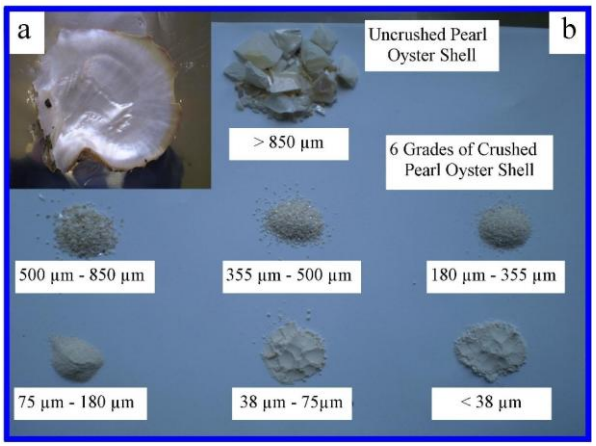

Figure 2. (a) *Pinctada Maxima* (pearl oyster) shells and (b) Various grades produced after sieving $CaCO_3$ powder (38 to 850 micrometers).

D. Preparation of Shell Substrates

The second part of the study used the shell as a substrate for the deposition of a HAP coating. The substrates were prepared by first pre-washing and cleaning the raw shells. After cleaning the shells were placed in a clean bench vice and cut into 1 cm^2 test substrates using a standard hacksaw (32 teeth per 25 mm). Substrates were then washed in running water in the lab sink to remove all cutting debris. In the next stage of cleaning samples were placed into a 250 ml beaker of Milli-Q® water then exposed to ultrasonic irradiation for 10 minutes to remove any loose particles that may have been embedded in the samples during the cutting stage. After the first irradiation, the Milli-Q® water was changed and the process repeated. In total, the samples were treated three times before being air dried and stored ready for surface treatment.

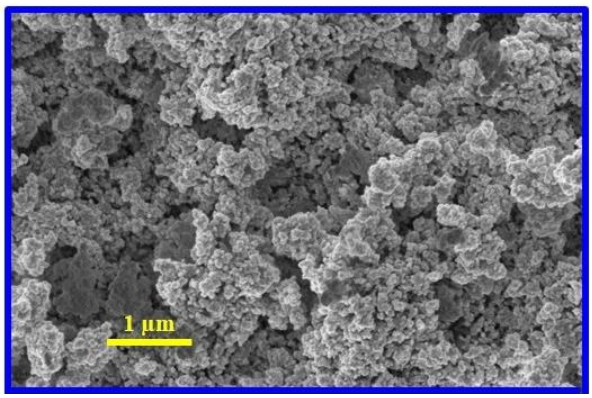

Figure 3. Figure 3 Representative *electron* microscopy image of HAP/$CaCO_3$ powder blend.

E. Subrate Surface Treatments and Coatings

A specific surface pre-treatment was applied to each respective substrate prior to coating. This was done to gauge the effectiveness of each surface pre-treatment in promoting coating attachment. Five pre-treatment procedures and an untreated substrate (control) were investigated and details of each pre-treatment are presented in Table I.

TABLE I. SUBSTRATE SURFACE PRE-TREATMENTS USED PRIOR TO COATING APPLICATION.

Substrate Type	Surface Treatment	Description
1	None (Control)	Sample is cleaned using Milli-Q® water and then air dried.
2	Chemical Hydrochloric Acid (HCl)	Sample is placed into a 500 ml beaker containing 200 ml of Milli-Q® water and 10 ml of 35% HCL. Solution pH was measured and found to be 1. The sample remains in the solution for 3 minutes. It is then removed and washed with Milli-Q® water and air dried.
3	Chemical Sodium Hypochlorate (SH)	Sample is place into a 500 ml beaker containing 200 ml of household bleach. (45g/l of sodium hypochlorate). The sample remains in the solution for 30 minutes. It is then removed and washed with Milli-Q® water and then air dried.
4	Boiling (B)	Sample is place into a 500 ml beaker containing 200 ml of Milli-Q® water and boiled for 10 minutes. It was then removed and washed with Milli-Q® water and then air dried.
5	Mechanical Abrasion (A)	Sample is roughened using silicon carbide sand paper (180p). 15 lateral movements followed by 15 vertical movements. The sample was then placed into a 500 ml beaker containing 200 ml of Milli-Q® water and exposed to 5 minutes of ultrasonic irradiation to remove any loose particles and contamination from the sand paper. The sample was then air dried.
6	Mechanical (S)	Sample is placed into a bench vice. The sample is scored by 20 lateral movements (both directions) by a surgical scalpel. The sample was then placed into a 500 ml beaker containing 200 ml of Milli-Q® water and exposed to 5 minutes of ultrasonic irradiation to remove any loose particles. The sample was then air dried.

The surface coating procedure consisted of using a spatula to evenly spread a layer of HAP powder over the surface of sample types 2 to 6, sample 1 being the unloaded control sample. After coating, all samples were placed into ceramic furnace boats and then individually placed into a pre-heated furnace set to 400°C. Samples remained in the furnace for 2 hours to calcify the coating in the presence of atmospheric air. After 2 hours of thermal treatment, the ceramic boats were removed from the furnace and allowed to cool down to room temperature in air.

F. Advanced Characterisation

Powder X-ray diffraction (XRD) spectroscopy was used to identify the crystalline size and phases present in synthesized HAP powders. Spectroscopy data was recorded at room temperature, using a Siemens D500 series diffractometer [Cu K_α = 1.5406 Å radiation source] operating at 40 kV and 30 mA. The diffraction patterns were collected over a 2θ range of 20 ° to 60 ° with an incremental step size of 0.04 ° using flat plane geometry with a 2 second acquisition time for each scan. The crystalline size of the particles was calculated using the Debye-Scherrer equation [Equation 1] from the respective spectroscopy patterns. Field emission scanning electron microscopy (FESEM) was also used to study size, shape and morphological features of the various powders. All micrographs were taken using a high resolution FESEM [Zeiss 1555 VP-FESEM] at 3 kV with a 30 μm aperture operating under a pressure of 1.333×10^{-10} mbar. Samples were mounted on individual substrate holders using carbon adhesive tape before being sputter coated with a 2 nm layer of gold to prevent charge build up using a Cressington 208HR High Resolution Sputter coater.

III. Results and Discussions

A. XRD Spectroscopy Analysis of Synthesised HAP Powders

XRD spectroscopy was used to identify the crystalline size of the synthesised nanometre scale HAP powders. A representative XRD pattern of a thermally treated HAP powder (400 ℃ for 2 h) is presented in Fig. 4. The pattern shows the main (h k l) indices found in the sample, namely (002), (211), (112), (300), (202), (310), (222), (213) and (004). These indices match the known phases present in pure HAP and are consistent with the phases listed in the ICDD database.

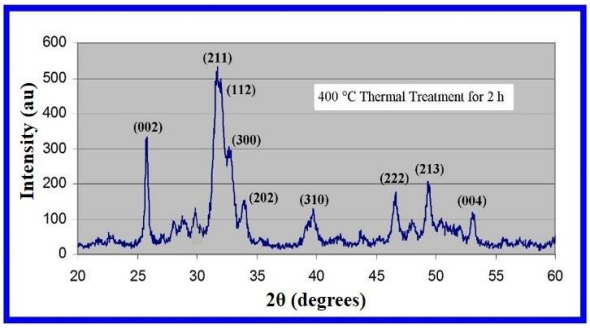

Figure 4. Representative XRD pattern of a HAP powder after thermal treatment.

The crystalline size, $t_{(hkl)}$, of each sample was calculated from the respective XRD patterns using the Debye-Scherrer equation [19], [20].

$$t_{(hkl)} = \frac{0.9\lambda}{B\cos\theta_{(hkl)}} \quad (1)$$

where, λ is the wavelength of the monochromatic X-ray beam, *B* is the Full Width at Half Maximum (FWHM) of the peak at the maximum intensity, $\theta_{(hkl)}$ is the peak diffraction angle that satisfies Bragg's law for the (h k l) plane and $t_{(hkl)}$ is the crystallite size. The crystallite size of each sample was calculated from the (002) reflection peak. HAP samples thermally treated at 400 ℃ gave a mean particle size of 30 nm.

B. FESEM Analysis of Pure and Blended Powders

FESEM was used to study particle size and morphology of the pure powders and blended powders. Representative micrographs of the synthesized powders are presented in Fig. 5 (a) to (d). Fig. 5 (b) reveals a spherical/granular particle morphology that is highly agglomerated and is typical of the synthesised HAP powder samples. Also present in Fig. 5 (b) are three 50 nm diameter circles placed randomly to highlight the spherical/granular morphology. This morphology is similar to particle morphologies previously reported in the literature [21-22].

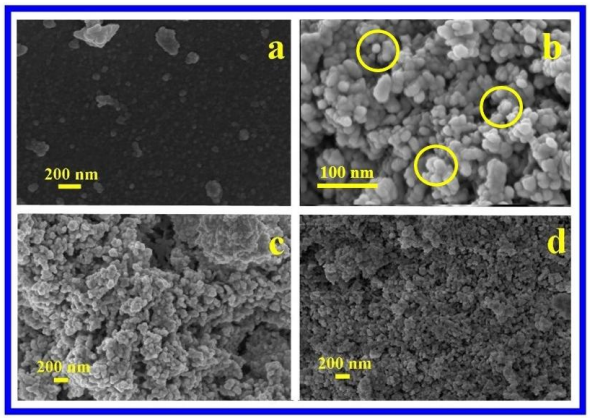

Figure 5. (a) Milled $CaCO_3$ powder sifted through a 38 micron sieve; (b) Pure ultrafine HAP powder; (c) HAP/$CaCO_3$ composite (5% $CaCO_3$ and particle sizes less than 38 micron) and (d) HAP/$CaCO_3$ composite (10 % $CaCO_3$ particle graded between 38 and 75 microns).

The raw $CaCO_3$ powder was sifted through a 38 micron sieve to produce a relatively homogeneous powder consisting of thin plates and finer granular shaped particles ranging in size from 20 to 100 nm as seen in Fig. 5 (a). A representative micrograph of a HAP/$CaCO_3$ composite (5%) is presented in Fig. 5 (c) and reveals the presence of granular shaped particles with pronounced edges that appear to be moderately packed and range in size from 50 to 100 nm. This is in stark contrast to the smooth and spherical HAP particle morphologies seen in Fig. 5 (b). Fig. 5 (d) presents a representative micrograph of a HAP/$CaCO_3$ (10%) and also reveals the presence of tightly packed granular particles. The particles range in size from 50 to 100 nm and have similar morphology to particles seen in the HAP/$CaCO_3$ (5%) composite. Analysis of FESEM micrographs taken of composite samples has confirmed the influence of $CaCO_3$ on particle morphology during the synthesis of the HAP composites.

C. Surface Pre-Treatments and Coating Attachment

The results of HAP deposition revealed some interesting surface features on the various substrates after thermal treatment. Initial inspection revealed lamellae from the inner white layers of the substrate had bubbled and broken away during calcification in the furnace. Substrate Type 1 (control) showed signs of surface bubbling and still retained its pearlescent lustre. The remaining 5 substrate types all exhibited a dull white coating that indicated HAP had adhered to the respective surfaces. Substrate Type 2 (HCl) showed signs of minor delaminating and on the whole HAP had adhered to the surface. Type 3 (SH) that had involved a bleaching process showed the most significant change. The surface had a distinctive white appearance with a significantly thicker and denser HAP coating compared to the other substrate types. Type 4 (B) that had involved a boiling treatment showed significant lamellae delaminating and also produced very brittle substrates. Overall, Type 4 produced poor quality substrates that were unsuitable for any tissue engineering applications. Both Type 5 (A) and Type 6 (S) revealed significant amounts of HAP had been trapped within the rough surface features created by the respective surface treatments. Surface scoring used in Type 6 trapped the largest amounts of HAP within the surface features and significantly contributed to coating integrity. Generally, both surface texturing techniques were found to be beneficial in promoting surface fixation of the coatings.

Subsequent FESEM surface studies of the various substrate types revealed some interesting surface features. In the case of Type 1 (control) there was tracing of HAP found, even though there was no HAP coating applied to the surface. The presence of distinct HAP particles over the entire face of the control substrate was found to be the result of ongoing calcification processes occurring within the furnace environment as seen in Fig. 6 (a). Both water and NH_4 evaporating from surrounding substrates tended to be deposit on everything within the furnace. Only Type 1 substrate showed this type of surface feature. Type 2 (HCl) substrate had a thick surface covering, unfortunately the coating was not uniformly distributed over the entire surface. There were numerous regions were the underlying lamellae structure could be seen as shown in Fig. 6 (b). Type 3 (SH) substrates were covered with a thick and dense white surface coating that was evenly distributed over the entire surface. Unlike Type 2, Type 3 substrates had a superior surface coverage with far fewer exposed underlining lamellae regions. Overall, FESEM analysis found HAP coating preferred to deposit and attach to the bleached surfaces of Type 3 substrates than those of the acid treated surfaces of Type 2 as seen in Fig. 6 (c) and 6 (d). In both cases, the mean HAP particle size for both substrate types determined from FESEM analysis was found to be 500 nm. The surface coverage on substrate types 5 and 6 were not thick or uniformly distributed. Instead they tended to accumulate HAP within and around the roughened surface features. On the whole, both substrate types had surfaces with poor coverage with large areas of underlining substrate clearly visible. However, further investigation is needed to fully investigate the effects of surface texturing, and in particular the effects of surface texturing before chemically treating the substrates with bleach. Bleaching substrates using the Type 3 (SH) method has proven to produce a superior HAP surface coating compared to other methods tested in this study. Future studies are planned to investigate the wear properties and load bearing capacity of the Type 3 (SH) substrates. In addition, *in vitro* studies are also planned to investigate the biocompatibility of the substrates towards a number of bone cell lines.

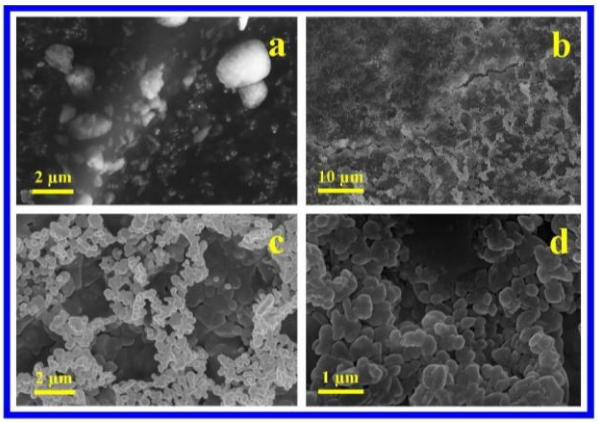

Figure 6. FESEM analysis of various substrate surfaces: (a) Substrate Type 1 (Control) showing the deposition of HAP particles during the calcination process; (b) Type 2 (HCl) showing minor delaminating of the thin HAP coating; (c) Type 2 (HCl) enlarged view of coating with underlying lamellae exposed, and (d) Type 3 (SH) substrate showing an evenly distributed thick coating over the entire substrate surface with far fewer exposed lamellae regions.

IV. Conclusion

HAP is a calcium phosphate that is considered to be a viable replacement for bone material in a number of low-load bearing tissue engineering applications. While the nacre layer found inside the *Pinctada maxima* (pearl oyster) shell is hard, stiff, and extremely tough. The present study has shown that a nanometre scale HAP powder (mean particle size of 30 nm) can be combined with sieved powders derived from *Pinctada maxima* ($CaCO_3$) to produce a composite powder. During synthesis, the addition of sieved powders were found to influence particle size and morphology of composite powders. The tough nacre was used as a substrate and a number of surface pre-treatments were investigated before the substrates were coated with HAP. The results of the investigation revealed a substrate pre-treated with sodium hypochlorate (Type 3) before HAP deposition produced the superior coating. The surface coating was thick, dense and evenly distributed. However, further studies are needed to investigate wear properties and load bearing capacities of the Type 3 substrate. Future *in vitro* studies are planned to determine the biocompatibility of the substrates towards a number of bone cell lines.

ACKNOWLEDGEMENTS

The authors would like to thank Dr Xuan Le for her assistance with FESEM analysis.

REFERENCES

[1] S. Weiner and H. D. Wagner, "The material bone: Structure-mechanical function relations," *Ann Rev Mater Sci.*, vol. 28, pp. 271-298, 1998.
[2] C. Hellmich and F. J. Ulm, "Average hydroxyapatite concentration is uniform in the extracollagenous ultrasturture of mineralized tissues: Evidence at the 1-10μm scale," *Biomechan Model Mechanobiol*, vol. 2, pp. 21-36, 2003.
[3] W. J. E. M. Habraken, J. G. C. Wolke, and J. A. Jansen, "Ceramic composites as matrices and scaffolds for drug delivery in tissue engineering," *Advanced Drug Delivery Reviews*, vol. 59, pp. 234-248, 2007.
[4] D. W. Hutmacher, J. T. Schantz, C. X. F. Lam, K. C. Tan, and T. C. Lim, "State of the art and future directions of scaffold-based bone engineering from a biomaterials perspective," *J. Tissue Eng. Regen. Med.*, vol. 1, pp. 245-260, 2007.
[5] M. Bonner and I. M. Ward, "Hydroyapatite/polypropylene composite: A novel bone substitute material," *J. Materials Science Letters*, vol. 20, no. 22, pp. 2049-2051, 2001.
[6] I. Ono, T. Tateshita, and T. Nakajima, "Evaluation of a high density polyethylene fixing system for hydroxyapatite ceramic implants," *Biomaterials*, vol. 21, pp. 143-151, 2000.
[7] J. D. Currey, "Mechanical properties of mother of pearl in tension," in *Proc. R. Soc.*, 1977, pp. 443-463.
[8] F. Barthelat, "Nacre from mollusk shells: A model for high-performance structural materials," *Bioinsp. Biomim.*, vol. 5, no. 035001, pp. 1-8, 2010.
[9] U. G. K. Wegst and M. F. Ashby, "The mechanical efficiency of natural materials," *Phil. Mag.*, vol. 84, pp. 2167-2181, 2004.
[10] S. Kamat, *et al.*, "Structural basis for the fracture toughness of the shell of the conch Strombus gigas," *Nature*, vol. 405, pp. 1036-1040, 2000.
[11] M. Rousseau, *et al.*, "Multi-scale structure of sheet nacre," *Biomaterials*, vol. 26, pp. 6254-6262, 2005.
[12] X. D. Li, *et al.*, "Nanoscale structural and mechanical characterization of a natural nanocomposite material: the shell of red abalone," *Nano Lett.*, vol. 4, pp. 613-617, 2004.
[13] M. Lamghari, *et al.*, "Stimulation of bone marrow cells and bone formation by nacre: in vivo and in vitro studies," *Bone*, vol. 25, pp. 91-94, 1999.
[14] L. P. Mouries, M. J. Almeida, C. Milet, S. Berland, and E. Lopez, "Bioactivity of nacre water-soluble organic matrix from the bivalve mollusk Pinctada Maxima in three mammalian cell types: Fibroblasts, bone marrow stromal cells and osteoblasts," *Comp. Biochem. Physiol. B.*, vol. 132, pp. 217-229, 2002.
[15] S. Berland, O. Delattre, S. Borzeix, Y. Catonne, and E. Lopez, "Nacre/bone interface changes in durable nacre endosseous implants in sheep," *Biomaterials*, vol. 26, pp. 2767-2773, 2005.
[16] K. S. Vecchio, X. Zhang, J. B. Massie, M. Wang, and C. W. Kim, "Conversion of bulk seashells to biocompatible hydroxyapatite for bone implants," *Acta Biomaterialia*, vol. 3, pp. 910-918, 2007.
[17] G. E. J. Poinern, R. Brundavanam, X. Le, S. Djordjevic, M. Prokic, and D. Fawcett, "Thermal and ultrasonic influence in the formation of nanometer scale hydroxyapatite bio-ceramic," *International Journal of Nanomedicine*, vol. 6, pp. 2083-2095, 2011.
[18] G. E. J. Poinern, R. Brundavanam, X. Le, P. K. Nicholls, M. A. Cake, and D. Fawcett, "The synthesis, characterisation and in vivo study of a bioceramic for potential tissue regeneration applications," *Scientific Reports*, vol. 4, no. 6235, pp. 1-9, 2014.
[19] H. P. Klug and L. E. Alexander, *X-ray Diffraction Procedures for Poly-Crystallite and Amorphous Materials.* 2nd Ed., New York, Wiley, 1974.
[20] C. S. Barrett, *et al.*, *Advances in X-ray Analysis*, New York: Plenum Press, 1986.
[21] Y. Han, S. Li, X. Wang, I. Bauer, and M. Yin, "Sonochemical preparation of hydroxyapatite nanoparticles stabilized by glycosaminoglycans," *Ultrasonics Sonochemistry*, vol. 14, no. 3, pp. 286-290, 2007.
[22] Z. H. Zhuo, P. L. Zhou, S. P. Yang, X. B. Yu, and L. Z. Yang, "Controllable synthesis of hydroxyapatite nanocrystals via a dendrimer-assisted hydrothermal process," *Materials Research Bulletin*, vol. 42, no 9, pp. 1611-1618, 2007.

R. K. Brundavanam, male, is presently working as a research associate at Murdoch Universities Nanotechnology laboratory. He holds a Master of Science (Physics) from Nagarjuna University, India and has recently completed his PhD research project entitled: Sonochemical synthesis, characterisation and biological evaluation of nanohydroxyapatite for potential hard tissue engineering applications at the Murdoch Applied Nanotechnology Research Group in Western Australia. His research interests include material science, nanomaterial synthesis and biomedical materials engineering and development.

D. Fawcett, male, is presently working as a research fellow at Murdoch Universities Nanotechnology laboratory. He holds a Ph.D. in Physical Sciences (Murdoch University) and Masters of Engineering from the University of Western Australia. He is an advanced-materials engineer, who interests are focused on developing biomedical materials, green synthesis of nanomaterials and the development of novel composites for applied applications.

G. E. J. Poinern, male, is currently a senior lecturer in physics and nanotechnology and director of the Murdoch Applied Nanotechnology Research Group, Murdoch University. He discovered and pioneered the use of an inorganic nanomembranes for potential skin tissue engineering applications and nanohydroxyapatite-based composites for bone tissue engineering. His research interests include: the green chemical synthesis of nanoparticles for use in biomedical, environmental remediation and photo-thermal applications.